INDIRECT DETECTION OF PERMAFROST DEGRADATION IN EASTERN ALASKA USING MODIS AND LANDSAT DATA

Kristie HU (China, PR), Masoume MAHBOUBI (Canada), Yiping CHEN (China, PR) and Sarah FATHOLAHI (Canada)

KEY WORDS: Satellite Remote Sensing, Permafrost, Land Surface Temperature, Vegetation Index, Eastern Alaska

ABSTRACT

Rising temperatures in polar regions due to climate change are causing significant changes in landscapes dominated by permafrost. The extent and severity of these changes have previously been hard to quantify due to the remote nature of the area of permafrost for the data collection process, but modern advances in satellite remote sensing technology have allowed a plethora of relevant data to be easily accessed and used for analysis. In this study, satellite imagery is used to detect changes in the landscape that indicate melting permafrost in Eastern Alaska. Three main metrics are the focus of the review: land surface temperature (LST), vegetation cover, and the annual maximum extent of water bodies. Indexes such as Normalized Difference Vegetation Index (NDVI), Enhanced Vegetation Index (EVI), and Modified Normalized Difference Water Index (MNDWI) are used to generate the results, culminating in a multivariate analysis of the change in permafrost in Eastern Alaska over the study period of 2000 – 2015. Results show that the vegetation greening trend in Eastern Alaska considering the overall change trend of EVI values are indicators of permafrost thawing in these years. Besides, based on Sen's slope, surface temperatures have been increasing over time, thus confirming that rising surface temperature is the driving force of permafrost melting.

Detection of Permafrost Degradation in Eastern Alaska Using Modis and Landsat Data (11672)
Kristie Hu (Canada), Yiping Chen (China, PR) and Sarah Fatholahi (Canada)

FIG Congress 2022
Volunteering for the future - Geospatial excellence for a better living
Warsaw, Poland, 11–15 September 2022

INDIRECT DETECTION OF PERMAFROST DEGRADATION IN EASTERN ALASKA USING MODIS AND LANDSAT DATA

Kristie HU (China, PR), Masoume MAHBOUBI (Canada), Yiping CHEN (China, PR) and Sarah FATHOLAHI (Canada)

1. INTRODUCTION

Permafrost is defined as ground that remains at or below 0°Cfor two or more consecutive years (Dobinski, 2011). In recent years, global warming in the polar regions is causing significant changes to areas consisting of permafrost. So, permafrost has begun to melt in polar regions worldwide. Permafrost contains large amounts of greenhouses gases that have accumulated in the soil due to the death and subsequent decomposition of living things. Methane (CH_4) and carbon dioxide (CO_2) are the two most common gases contained in permafrost, with billions of tons stored and millions of tons released annually due to melting (Shakhova et al., 2012; Natali et al., 2012).After release into the atmosphere, these greenhouse gases enhance the atmosphere's ability to retain heat, further increasing atmospheric temperatures and encouraging further melting of permafrost, creating a dangerous feedback loop that can cause climate change to rapidly accelerate (Adiya, et al., 2021). Another potential concern is the mobilization of dissolved organic compounds and other materials such as soil nutrients within freshwater systems as they are released due to the melting of permafrost. For example, large amounts of ammonium could be released (Fouché, et al., 2020), causing pH imbalances downstream and potentially creating inhospitable environments for local flora and fauna, leading to an ecosystem collapse. Permafrost thawing is a geological change that will directly affect the future trend of the entire climate change. Hence, understanding land surface changes in permafrost regions is critical to climate change mitigation strategies related to permafrost degradation. The nature and extent of the changes of permafrost are complicated by ecological responses on strong gradients in environmental conditions and within the perturbation range. Emerging remote sensing technologies, based on an increasing number of satellite and airborne platform arrays, are covering an increasingly wide range of time as well as space and are highly capable of reliably monitoring changes in permafrost landscapes (Jorgenson, et al., 2016). There is currently data that supports that climate change and changing disturbance mechanisms are causing permafrost degradation. The change of lake area is one of the effects of permafrost degradation, affecting the distribution and availability of water resources in the future. One such example is that changes in lakes can affect the level of water in soils, causing surface flora such as trees to die once the ground reaches a point of oversaturation. Furthermore, draining water can cause flooding, excessive erosion (e.g., landslides, sinkholes), and other unwanted side effects further downstream (Jorgenson, et al., 2001). One of the objectives of this research is to investigate if the changes in vegetation cover over time observed in the study region were consistent with changes expected in regions experiencing permafrost degradation. A study performed based on land cover changes in Quebec, Canada, have been quantified to estimate changes in permafrost that produce discontinuous changes to the forest-tundra transition zone,

Detection of Permafrost Degradation in Eastern Alaska Using Modis and Landsat Data (11672)
Kristie Hu (Canada), Yiping Chen (China, PR) and Sarah Fatholahi (Canada)

FIG Congress 2022
Volunteering for the future - Geospatial excellence for a better living
Warsaw, Poland, 11–15 September 2022

it also presented an overall increase in vegetation between 1986 and 2009, while high vegetation increased by 21% between 2004 and 2009 (Beck et al., 2015). It demonstrates the feasibility of using high-resolution satellite imagery to detect land surface changes that can be used as subarctic permafrost degradation indicators. Research shows that one of the major signals of permafrost thaw is related to the changes in vegetation cover, more specifically its expansion. Indeed, greening in permafrost regions is a response to warming temperatures that imply warming permafrost. The greening in association with thawing permafrost is likely due to the increasing thawing index, which provides more heat for the growth of plants, moreover, there is a positive correlation between the thawing index and the Normalized Difference Vegetation Index (NDVI), which suggests that warming permafrost may encourage vegetation growth (Peng et al., 2020). The thawing index is an indicator used in estimating the depth of the active layer in permafrost regions. Furthermore, research shows that increase in the depth of the active layer of permafrost is generally tied to wetter soil conditions that are associated with nutrient-rich plant growth (Christensen et al., 2004). It is important to note that there are various factors at play in the dynamics of permafrost change that are beyond the scope of this research. One of these major factors is climatic conditions that need to be taken into consideration as it plays a major role in both vegetation change and permafrost thaw. Vegetation indexes of NDVI and Enhanced Vegetation Index (EVI) take advantage of the spectral signatures of vegetation. Vegetation absorbs radiation in the blue and red wavelengths and reflects in the green band with far greater reflectance in the near-infrared (NIR) band, reflectance in the NIR band is pivotal for qualitative and quantitative assessment of vegetation. Spectral signatures of vegetation area are impacted by various factors such as water content, plant type, leaf chlorophyll concentration, leaf area index (LAI) among others. The spongy mesophyll layer in the leaf surface has a high reflectivity in the NIR band and low reflectance in the visible bands (blue and red wavelengths). Furthermore, a study conducted in Arctic tundra landscapes reveals that there exists a high potential to use land surface temperature (LST) anomalies to detect land cover changes in these areas because of permafrost degradation or climate change (Muster et al., 2015).

2. RELATED WORK

Several research papers address the melting problem of permafrost through different analytical methods. Research conducted suggests that the response of northern tundra plant communities to warming is critical and permafrost ecosystems play a crucial role in global carbon storage, and climate-induced changes in permafrost will affect organisms and their direct carbon dioxide transfer (Natali et al., 2012). Bui et al. (2020) estimated accuracy and limitations of different hydrological models for the analysis of hydrological processes of permafrost in the Arctic region. In another research sensitivity and robustness of satellite data of MODIS to the LST changes in different land covers in the Canadian Arctic region have been analyzed, and their validation with in-situ radiometer measurements have been taken into account, and as a result, high anomalies and variations in spatial and temporal scales have been observed (Muster et al. 2015). With the same token, Hachem et al. (2012) demonstrated the correlation between MODIS LST and ground surface temperature and near-surface air temperature in the permafrost zone, which showed a strong correlation in snow-covered time of the year, pinpointing on the fact that LST is a crucial indicator of land cover changes in the permafrost region. Beck et al.

Detection of Permafrost Degradation in Eastern Alaska Using Modis and Landsat Data (11672)
Kristie Hu (Canada), Yiping Chen (China, PR) and Sarah Fatholahi (Canada)

FIG Congress 2022
Volunteering for the future - Geospatial excellence for a better living
Warsaw, Poland, 11–15 September 2022

demonstrated the utilization of other satellite data including Landsat and QuickBird, to discover the land cover changes, focusing on vegetation and water covers, as an indicator of permafrost degradation. Boike e al. (2016) performed research based on using MODIS and Landsat images to explore changes in water bodies, LAI, LST, and forest fires frequency and intensity, and the results have shown a continuous warming pattern. Carpino et al. (2018) also performed a change detection analysis of forest covers for the first time on a large scale in the permafrost area and Du et al. (2016) illustrated the utilization of Sentinel-2 data for extraction of indices such as Normalized Difference Water Index (NDWI) and Modified NDWI (MNDWI), the research takes advantage of 4 pan-sharpening algorithms to use the best possible spatial resolution from Sentinel-2 data to acquire accurate information about water bodies coverage. However, Gao et al. (2020) stated the fact that due to limitations of optical remote sensing for inside permafrost analysis, dual-index algorithm (DIA) coupled with permafrost classification method is more beneficial. Peng et al. (2015) and Gandhi et al. (2015) performed change detection by NDVI differencing to explore changes of different land covers and greening trends. Instead of NDVI, Singh et al. (2015) utilized NDWI and MNDWI indexes to detect waterlogging from ResourceSat-2 AWiFS satellite data. Using satellite data and airborne geophysical surveys, Jepsen et al. (2013) determined the relationship between permafrost and water areas changes, focusing on the fact that shallow part of permafrost is more influential than deeper parts in the distribution of lakes in the interior Alaska. Jorgenson & Grosse (2016) discussed the possibility of fusion of different data sources such as InSAR, LiDAR and airborne geophysics to determine changes in landscape media such as thermokarst lakes and drained lake basins, as indicators of the permafrost degradation.

Kääb (2008) performs a hazard analysis using SAR and LiDAR data as well as the digital elevation models (DEMs) in the cryosphere hazard zones resulting from massive permafrost movements and unstable slopes. With the same token, Kääb, et al. (2005) represented a comprehensive overview of remote sensing techniques coupled with GIS for risk and permafrost-related hazard assessment in the mountain area. Natali et al. (2011) experiment two kinds of winter and summer warming into the soil and permafrost and explore the productivity of tundra plants, the results of which were increased biomass in winter and prolonged growing season in both winter and summer. In the study of Nguyen et al. (2009), SPOT-5 data and the supervised maximum-likelihood classification (MLC) were used to determine riparian area extent and as a result the depth of permafrost zone, which had more accurate results than most permafrost maps in Canada. In the study of Nill et al. (2019), LST changes were analyzed using Landsat data accompanied by NDVI, NDWI, Tasseled Cap greenness (TCG), brightness (TCB), and wetness (TCW), and DEMs, and Theil-Sen (T-S) regression method has been taken into account to explore the relationship between indexes and LST. Novikova et al. (2018) utilized multi-temporal aerial and satellite imagery to find out the planimetric and volumetric retreat rates of permafrost. Nyland et al. (2018) proposed a semi-automated Random Forest classification technique using optical imagery available on Google Earth Engine, the result of which is increasing greening trend and decreasing water areas indicating permafrost degradation. Panuju et al. (2020) applied satellite multispectral data to analyze the change detection direction and magnitude, its probability and frequency in land cover. Park et al. (2016) utilized satellite microwave observations for the first time for permafrost extent analysis using freeze-thaw (FT) status.

Detection of Permafrost Degradation in Eastern Alaska Using Modis and Landsat Data (11672)
Kristie Hu (Canada), Yiping Chen (China, PR) and Sarah Fatholahi (Canada)

FIG Congress 2022
Volunteering for the future - Geospatial excellence for a better living
Warsaw, Poland, 11–15 September 2022

Pastick et al. (2013) implemented a regression and extrapolation based on decision trees using electromagnetic resistivity data and Landsat TM and DEMs to demonstrate the permafrost mapping and monitoring. By a similar approach Sarp & Ozcelik (2017) used Support Vector Machine (SVM) beside indexes to extract water area from Landsat TM and ETM+ imagery. Permafrost degradation is also of critical importance for Greenhouse Gas Emissions. (Christensen, et al., 2004) demonstrate how changes in permafrost coverage can increase Greenhouse gas emissions. (Fouché, et al., 2020) examines 25 soil cores from 9 different sites in Canadian Arctic to understand dissolved organic carbon and nitrogen stocks mobilization inside the thawing permafrost into watersheds. There are several possibilities to explore the trend and pattern in LST and its relationship with permafrost degradation. Exercise of Mann-Kendall and Sen's methods have been explored in several studies, for instance, Gocic et al. (2013) used them to determine the trend in several meteorological variables such as temperature, relative humidity, vapor pressure, and precipitation. Mustapha (2013) utilized the Mann-Kendall test and Sen's Slope estimator for homogeneous trend direction detection and intensity based on eight different physicochemical and precipitation indicators in the river basins. Li et al. (2021) exercised ENVISAT ASAR data for deformation detection and Zhang et al. (2021) explored efficacy of WorldView-2 for analysis of active layer of permafrost.

3. STUDY AREA AND METHOD

3.1. Study Area

The study area lays between Fort Yukon and Fairbank in Eastern Alaska, USA (Figure 1). This inland area is located in the continental subarctic region, which is covered with a large amount of continuous as well as discontinuous permafrost all year round. The typical climate for our study area has long cold winters and short warm summers, with the lowest temperature ranging from -30°C in winter and to -15°C in summer (The Alaska Climate Research Center, 2018). Studies have shown that permafrost degradation is severe in inland Alaska causing shifts in land cover types (Jorgenson et al., 2001). Since one of our study objectives is to detect how the land cover feature changes related to the permafrost degradation, a region that has a sufficient amount of vegetation cover, water bodies, as well as different landforms (for temperature comparing purposes) has been selected.
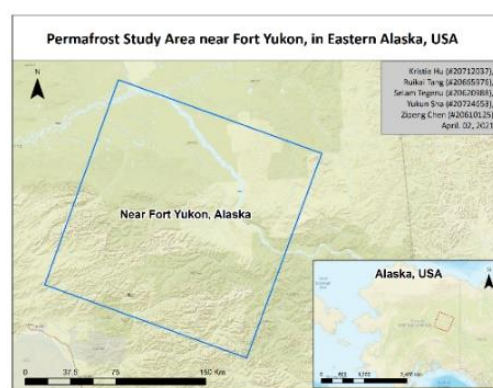

Figure 1. Our Proposed Study Area in Eastern Alaska, USA

Detection of Permafrost Degradation in Eastern Alaska Using Modis and Landsat Data (11672)
Kristie Hu (Canada), Yiping Chen (China, PR) and Sarah Fatholahi (Canada)

FIG Congress 2022
Volunteering for the future - Geospatial excellence for a better living
Warsaw, Poland, 11–15 September 2022

3.2. Enhanced Vegetation Index

The enhanced vegetation index (EVI) is a remotely sensed index that is widely used to monitor the conditions of vegetation by estimating the chlorophyll content of leaves. This index was obtained from the MOD13Q1.006 dataset for the past 20 years (2000 - 2020) in Eastern Alaska. EVI is similar to NDVI in that it can quantify the greenness of vegetation. Moreover, EVI corrects for changes in solar incidence angle, atmospheric conditions, canopy background noise, and offers higher sensitivity in areas with dense vegetation, and provides a more accurate and consistent estimate of greenness (USGS, 2021). EVI is calculated by

$$EVI = G \times \frac{(NIR-RED)}{(NIR+C1 \times RED-C2 \times BLUE+L)} \qquad (1)$$

where G is the gain factor (2.5), L is the adjustment for canopy background, C1, C2 are the coefficients of the aerosol resistance, uses the blue band to correct for aerosol influences in the red band, NIR is the near-infrared surface reflectance, RED and BLUE represent the reflectance in the red and blue bands. The Blue band removes residual atmosphere contamination caused by smoke and sub-pixel thin cloud clouds.

3.3. Change in Land Surface Temperature

Land surface temperature (LST) data derived from MODIS satellites were used to design a methodology for time series analysis of LST. The MOD11A2.006 Terra LST and Emissivity 8-day global 1 km is comprised of an 8-day composite of 1–2-day observation intervals and has a spatial resolution of 1 km. This data also covers our temporal range since it is available from March 2000 to the present. The Mann-Kendall statistical test has been widely used to investigate trends in hydro-meteorological time series (Gocic et al., 2013). Hence it is one of the popular non-parametric tests used to detect trends in time series data and it is possible to determine the presence of an increasing or decreasing trend as this test is less likely to be impacted by outliers. This is because it is not directly based on the values of the random variables but instead is based on the sign differences (Mustapha, 2013). In this study, the Mann-Kendall trend test examines every pair of the pixel value to determine the trend of the data over the years 2000 – 2020, which can be calculated by

$$S = \sum_{i=1}^{n-1} \sum_{j=i+1}^{n} Sign(T_j - T_i) \qquad (2)$$

$$Sign(T_j - T_i) = \begin{cases} 1 & \text{if } T_j - T_i > 0 \\ 0 & \text{if } T_j - T_i = 0 \\ -1 & \text{if } T_j - T_i < 0 \end{cases} \qquad (3)$$

where, a positive value of S indicates that there is an increasing trend; A negative value of S indicates that there is a decreasing trend in the time series. A zero-value indicated that there is no trend. Furthermore, Sen's Slope estimator is a non-parametric model used to determine the

Detection of Permafrost Degradation in Eastern Alaska Using Modis and Landsat Data (11672)
Kristie Hu (Canada), Yiping Chen (China, PR) and Sarah Fatholahi (Canada)

FIG Congress 2022
Volunteering for the future - Geospatial excellence for a better living
Warsaw, Poland, 11–15 September 2022

slope of the time series trend in both EVI and LST. This obtains the slope value for every pair of pixels in which the pixel pairs are comprised of values computed at time i, and another at j, where j represents a later time and i represent an earlier time.

$$Q_i = \frac{x_j - x_k}{j - k} \ for \ i = 1, \ ..., \ N, \qquad (4)$$

where x_j and x_k represent the data values at times j and k *where $j > k$*, respectively. N is a sample of N pairs of land surface temperature data, and Q_i is the value of the slope. These N slope values Q_i are ranked to determine the median to obtain Sen's slope as shown

$$Q_{med} = \begin{cases} Q_{(\frac{N+1}{2})} & \text{if N is odd} \\ \frac{Q_{(\frac{N}{2})} + Q_{(\frac{N+2}{2})}}{2} & \text{if N is even} \end{cases} \qquad (5)$$

The magnitude of Q_{med} indicates the slope of the trend while the sign indicates whether the trend is increasing, decreasing or if it has no change. The Sen's slope estimator was applied to variables of land surface temperature measured in degrees Celsius and maximum enhanced vegetation index for the summer months.

3.4. Change in Maximum Annual Extent of Water Bodies

Changes in the maximum annual extent of water bodies in Eastern Alaska can be linked to permafrost degradation. This research focuses on all bodies of water on the surface, including temporary melt ponds as well as permanent lakes, within the study area that has exhibited change over time. MNDWI analysis was chosen as our tool of choice due to its superior ability to delineate water features mixed with vegetation in comparison to NDWI (Singh et al., 2015; Xu, 2006). The changes observed may include both shrinkage and expansion of the maximum annual extent of water bodies. MNDWI composites will be generated for 5 years periods from 2000 to 2020, and then image differencing will be performed on these composites to show changes between these years. For Landsat 7 data, MNDWI is defined using the following bands

$$MNDWI = \frac{Band \ 2 - Band \ 5}{Band \ 2 + Band \ 5} \qquad (6)$$

where Band 2 and Band 5 respectively represent the green band (0.52 – 0.60 µm) and the SWIR band (1.55 – 1.75 µm) of Landsat 7 ETM+. The output is a number in between -1 and 1, with negative values showing evidence for the non-water surfaces and positive values showing evidence for water surfaces, with evidence becoming stronger as the value moves away from 0.

Detection of Permafrost Degradation in Eastern Alaska Using Modis and Landsat Data (11672)
Kristie Hu (Canada), Yiping Chen (China, PR) and Sarah Fatholahi (Canada)

FIG Congress 2022
Volunteering for the future - Geospatial excellence for a better living
Warsaw, Poland, 11–15 September 2022

3.5. Normalized Difference Vegetation Index

Permafrost degradation in Eastern Alaska can be linked to changes in the vegetation cover. Except for EVI, NDVI analysis also was employed to look at changes in vegetation within the study area over the given study period. Both increases and decreases in vegetation are expected in different areas. NDVI composites will be generated for 5 years periods from 2000 to 2020, and then image differencing will be performed on these composites to show changes between these years. For Landsat 7 ETM+ data, NDVI is defined as

$$NDVI = \frac{Band\ 4 - Band\ 5}{Band\ 4 + Band\ 5} \qquad (7)$$

where Band 4 and Band 5 respectively represent the NIR band (0.77 – 0.90 µm) and the SWIR band (1.55 – 1.75 µm) of Landsat 7 ETM+. The output is a number in between -1 and 1, with negative values showing evidence for a lack of vegetation present on surfaces and positive values showing evidence for vegetation presence on surfaces, with evidence becoming stronger as the value moves away from 0.

3.6. Maximum-Likelihood Supervised Classification

The supervised classification analysis gives us a comprehensive overview of how the different land cover features are distributed within our study area. By classifying the features from each 5-year-time interval image, we can compare the changes over time and interpret how different land feature change pattern looks like. On the other hand, by comparing the classification result to the EVI, NDVI, MNDWI, and LST analysis result, we can effectively evaluate the analysis results and detect any potential errors that could be generated during the processing on Google Earth Engine. We planned to perform this supervised classification to the data downloaded from USGS. As shown in Figure 2, we classified all the land features within the study area into 4 classes: water (blue), vegetation (light green), fallow field (yellow), as well as dense forest (dark green). After we collected sufficient sample data, we performed the maximum likelihood classification by running the tool. Lastly, we exported the output data once we ensure that our classification's accuracy level shows in the classification report turned to around 90%, which is a highly accurate classification.

4. RESULTS AND DISCUSSION

4.1. Changes in Vegetation Cover

Figure 2. Examples of sample training data

Detection of Permafrost Degradation in Eastern Alaska Using Modis and Landsat Data (11672)
Kristie Hu (Canada), Yiping Chen (China, PR) and Sarah Fatholahi (Canada)

FIG Congress 2022
Volunteering for the future - Geospatial excellence for a better living
Warsaw, Poland, 11–15 September 2022

The Mann-Kendall trend test applied to maximum EVI for summer produced the signs of maximum EVI pixels and a histogram showing their subsequent frequency as shown in Figure 3. This histogram shows the vast majority of the pixels in the study area depict positive trends over the years 2000 to 2020. The signs of the slopes were further used to infer vegetation conditions in the study area over time. The result from Sen's slope of maximum summer EVI further quantifies the changes in vegetation over the 20 years during the study period and it depicted a significant proportion of the study region exhibiting positive slope over the years 2000 to 2020. Sen's slope uses the median of the slopes from pairs of EVI data in the time series to detect changes. In this research both increase and decrease in Sen's slope indicated subsequent increase and decrease in summer EVI trends over the study period. This translates into a greening and browning trend in vegetation cover within the study region. However, the large proportion of this change involved greening over the years. Although decreasing trend of maximum summer EVI was far less in proportion than its increase, there was still a significant browning trend in certain areas of the study region particularly pronounced between 2005 - 2010. Map of the study area showing the slope values over time (in years) is presented in the following (Figure 4) and quantities such as areas impacted by increasing and decreasing EVI trends in km^2 are reported in Table 1.

Table 1. The total area under greening and browning measured in km^2, as well as the associated fractions of greening and browning areas within the study area

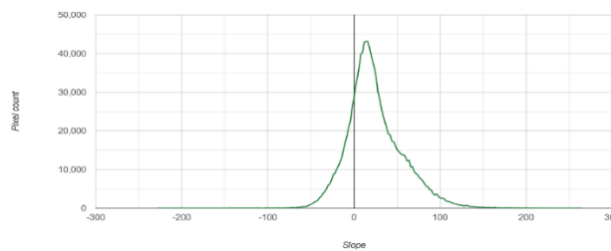|	Areas of Vegetation Greening and Browning		
Greening (sq km)	Greening fraction	Browning (sq km)	Browning fraction
26,498.21	0.82	6,028.56	0.187

Figure 3. Histogram of regression slope values showing positive and negative slope frequency of pixels of maximum summer EVI between 2000 - 2020

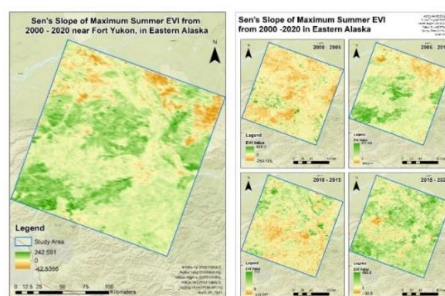**4.2. Changes in Maximum Annual Extent of Water Bodies**

Figure 4. Sen's slope of maximum summer EVI over time depicting areas with greening and browning trends between 2000 – 2020, and 5-year intervals.

Detection of Permafrost Degradation in Eastern Alaska Using Modis and Landsat Data (11672)
Kristie Hu (Canada), Yiping Chen (China, PR) and Sarah Fatholahi (Canada)

FIG Congress 2022
Volunteering for the future - Geospatial excellence for a better living
Warsaw, Poland, 11–15 September 2022

While there were always increasing and decreasing extents in different areas for consecutive 5-year periods, there was no obvious pattern. However, performing the image differencing between the first and last 5-year periods magnifies the pattern and makes the difference more noticeable. As shown in Figure 5, the net change in extent is positive. This means that the number of pixels representing an increase in water extent outnumbered the number of pixels representing a decrease. This is indicative of more permafrost melting in the later years of the study period as melting permafrost leads to large temporary bodies of water that show up when looking at a maximum annual extent that would be otherwise undetected if only permanent bodies of water were studied. The total net increase in maximum water extent is around 1.08% of the total area, implying that there is a not-insignificant degree of detectable permafrost melting that occurred over the study period as measured using this method. Thus, the most logical conclusion is that this result is evidence that supports the hypothesis that there is an increase in permafrost melting in our study area as measured by changes in the extent of water bodies, fulfilling the first research objective of understanding and quantifying the change in the maximum annual extent of water bodies in Eastern Alaska over time.
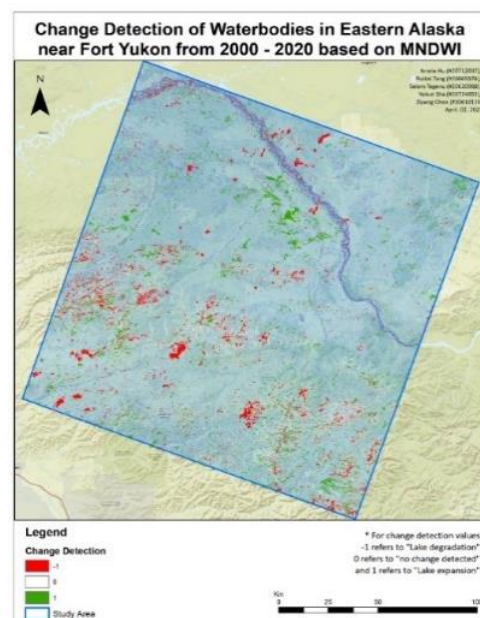

Figure 5. Changes in the maximum extent of water bodies between 2000 – 2020

4.3. Changes in LST

In this research, change detection of land surface temperature was performed through the estimation of Sen's slope. The areas showing a rise in land surface temperature over 20 years are major drivers of permafrost degradation in the study region. Research shows that surface temperature is the major climatic factor that governs the spatial distribution, existence, as well as thermal regime of permafrost (Hachem et al., 2012). Therefore, an increase and decrease in LST are critical in stimulating permafrost dynamics in the study region. However, it is important to note that other environmental factors play a key role in surface energy dynamics.

Detection of Permafrost Degradation in Eastern Alaska Using Modis and Landsat Data (11672)
Kristie Hu (Canada), Yiping Chen (China, PR) and Sarah Fatholahi (Canada)

FIG Congress 2022
Volunteering for the future - Geospatial excellence for a better living
Warsaw, Poland, 11–15 September 2022

Surface albedo is impacted by various factors such as clouds, aerosols, ice among others. However, this research focuses on LST changes only about permafrost degradation. Areas showing temperature rise over the study period are major signals of thawing permafrost trends. Research shows that LST can be used to detect land cover changes in Arctic tundra landscapes as a result of permafrost degradation as well as climate change (Muster et al., 2015). Therefore, it would be scientifically reasonable to predict that the areas experiencing an increase in LST in the study region over the 20 years temporal range are likely to experience permafrost degradation. Average LST data of summer months (June and July) was graphed for the study period as shown in Figure 6. Although the trend depicted in this graph does not show an overall increase or decrease over the years, there are certainly increasing and decreasing trends in certain areas within the study area over the years. These changes were determined by the result of the Mann-Kendall Trend test and its sign and Sen's slope estimator as shown in the maps in Figure 7. The maps shown in Figure 7 depict the areas that exhibited positive values of Sen's slope and those that exhibited negative values.
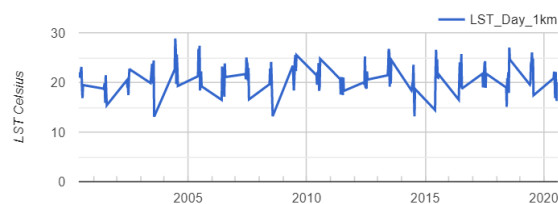

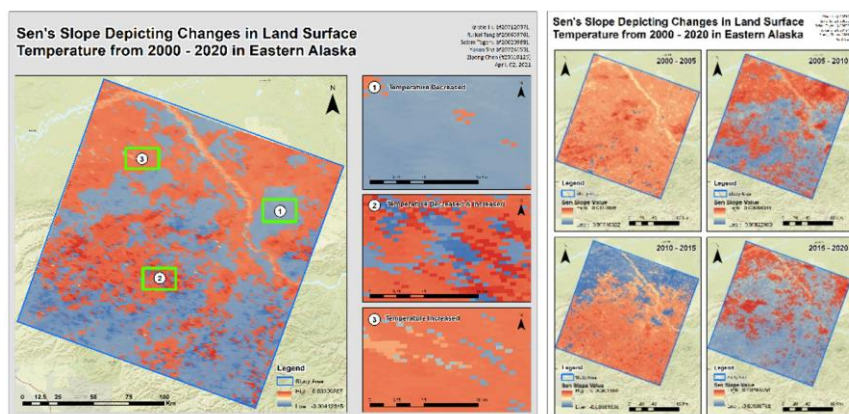**Figure 6**. Trends of summer average LST between 2000-2020

Figure 7. Maps depicting Sen's slope of summer land surface temperature show the sign and magnitude of the slopes (red: an increase in slope values, blue: a decrease).

4.4. Supervised Classification

Changes during the years 2000 to 2020 can also be easily detected by MLC in Figure 8. The land cover features within our study area have been classified into 4 classes (water, vegetation, dense vegetation as well as fallow field), blue refers to a waterbody, light green refers to vegetation, dark green refers to dense vegetation and yellow refers to the fallow field. The vegetation/water expansion (deduction) is indicated as the green/ blue area increase or

Detection of Permafrost Degradation in Eastern Alaska Using Modis and Landsat Data (11672)
Kristie Hu (Canada), Yiping Chen (China, PR) and Sarah Fatholahi (Canada)

FIG Congress 2022
Volunteering for the future - Geospatial excellence for a better living
Warsaw, Poland, 11–15 September 2022

decreases. Overall, from 2000 to 2020, the detected vegetation expansion is more than the vegetation deduction. Similarly, the expanded extent of the water bodies is more than the reduced extent of the water bodies.
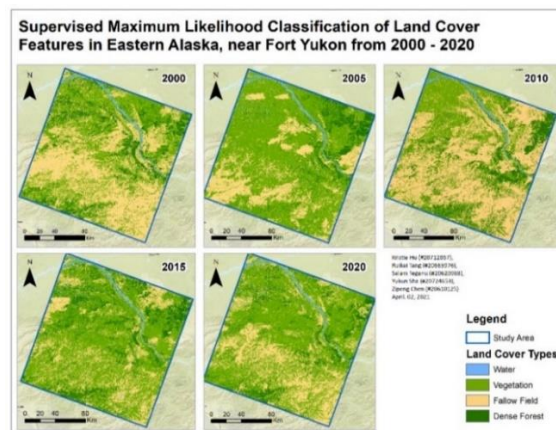

Figure 8. Supervised classification of land cover features in Eastern Alaska between 2000 – 2020

5. CONCLUSIONS

This paper focuses on use of satellite data to comprehensively analyze the changes of permafrost landscape from different aspects by extrapolation of changes in permafrost by analysis of vegetation, surface temperatures, and lake changes in Eastern Alaska. Landsat and MODIS data were used in this research to analyze and evaluate the study area. In addition, this research utilized NDVI, EVI, LST, and NDWI/MNDWI to analyze permafrost changes in Eastern Alaska from 2000 to 2020 on a 5-year basis. The results show that the vegetation greening trend in Eastern Alaska between 2000 to 2020 is the main indicator of permafrost thawing and the change of vegetation coverage in the EVI, NDVI, and MLC analysis provides the conclusion that the vegetation coverage in Eastern Alaska experiences an increasing trend between 2000 - 2020. Moreover, rising LST are bound to accelerate the degradation of permafrost. LST trends from 2000 to 2020, plotted using Sen's slope, show that LST have been increasing over time, thus confirming that rising LST is the driving force of permafrost melting.

In the future, we will explore the impact of permafrost melting and the countermeasures. Since permafrost contains a lot of greenhouse gases, of which CO_2 and CH_4 are the two most common, thawing permafrost means further warming of the atmosphere and further melting of the permafrost, creating a vicious cycle (Natali et al., 2012). Besides, the chain reaction of permafrost thawing on the ecological environment will become the main direction of the experimental project. Furthermore, the exercise of machine learning techniques such as Random Forest and Artificial Neural Networks (ANNs) may increase the accuracy of land cover detection and help to establish a stronger relationship between land cover changes and permafrost degradation. The current study can analyze features on the surface to find out what is happening in the underground world, as changes in the underground are reflected on the surface. However, future study will need to bring in more indicators and more 3D modeling techniques to take a deeper look at permafrost. Additional geophysical analysis of the

Detection of Permafrost Degradation in Eastern Alaska Using Modis and Landsat Data (11672)
Kristie Hu (Canada), Yiping Chen (China, PR) and Sarah Fatholahi (Canada)

FIG Congress 2022
Volunteering for the future - Geospatial excellence for a better living
Warsaw, Poland, 11–15 September 2022

permafrost using Ground Penetrating Radar (GPR) and electrical resistivity tomography alongside with geospatial data can provide more accurate data from underground permafrost features and thawing status (Kim et al., 2021; Li et al., 2021).

ACKNOWLEDGEMENTS

REFERENCES

Adiya, S., Dalantai, S., Wu, T., Wu, X., Yamkhin, J., Bao, Y., . . . Dorjgotov, B. 2021. Spatial and temporal change patterns of near-surface CO_2 and CH_4 concentrations in different permafrost regions on the Mongolian Plateau from 2010 to 2017, *Science of The Total Environment, 800*(149433).

Beck, I., Ludwig, R., Bernier, M., Lévesque, E., & Boike, J. 2015. Assessing permafrost degradation and land cover changes (1986–2009) using remote sensing data over Umiujaq, Sub-Arctic Québec. *Permafrost and Periglacial Processes* 26, 129-141.

Boike, J., Grau, T., Heim, B., Günther, F., Langer, M., Muster, S., Lange, S. 2016. Satellite-derived changes in the permafrost landscape of central Yakutia, 2000–2011: Wetting, drying, and fires. *Global and Planetary Change 139*, 116-127.

Bui, M. T., Lu, J., & Nie, L. 2020. A review of hydrological models applied in the permafrost-dominated arctic region. *Geosciences* 10(10) , 401.

Carpino, O. A., Berg, A. A., Quinton, W. L., & Adams, J.R. 2018. Climate change and permafrost thaw-induced boreal forest loss in northwestern Canada. *Environmental Research Letters*, 13, 084018

Christensen, T. R., Johansson, T., Åkerman, H. J., Mastepanov, M., Malmer, N., Friborg, T., . Svensson, B. H. 2004. Thawing sub-arctic permafrost: Effects on vegetation and methane emissions. *Geophysical Research Letters*, 13, 084018

Dobinski, W. 2011. Permafrost. *Earth-Science Reviews, 108*(3), 158-169.

Du, Y., Zhang, Y., Ling, F., Wang, Q., Li, W., & Li, X. 2016. Water bodies' mapping from Sentinel-2 imagery with modified Normalized Difference Water Index at 10-m spatial resolution produced by sharpening the SWIR band. *Remote Sensing 8(4)*, 354.

Fouché, J., Christiansen, C. T., Lafrenière, M. J., Grogan, P., & Lamoureux, S. F. 2020. Canadian permafrost stores large pools of ammonium and optically distinct dissolved organic matter. *Nature Communications, 11*(1), 4500-4500.

Gandhi, G. M., Parthiban, S., Thummalu, N., & Christy, A. 2015. NDVI: Vegetation change detection Using remote sensing and GIS – A case study of Vellore District, *Procedia Computer Science (57)*, 1199-1210.

Detection of Permafrost Degradation in Eastern Alaska Using Modis and Landsat Data (11672)
Kristie Hu (Canada), Yiping Chen (China, PR) and Sarah Fatholahi (Canada)

FIG Congress 2022
Volunteering for the future - Geospatial excellence for a better living
Warsaw, Poland, 11–15 September 2022

Gao, H., Nie, N., Zhang, W., & Chen, H. 2020. Monitoring the spatial distribution and changes in permafrost with passive microwave remote sensing. *ISPRS Journal of Photogrammetry and Remote Sensing 170*, 142-155.

Gocic, M., & Trajkovic, S. 2013. Analysis of changes in meteorological variables using Mann-Kendall and Sen's slope estimator statistical tests in Serbia. *Global and Planetary Change 100*, 172-182.

Hachem, S., Duguay, C. R., & Allard, M. 2012. Comparison of MODIS-derived land surface temperatures with ground surface and air temperature measurements in continuous permafrost terrain. *The Cryosphere 6*, 51-69.

Jepsen, S. M., Voss, C. I., Walvoord, M. A., Minsley, B. J., & Rover, J. 2013. Linkages between lake shrinkage/expansion and sublacustrine permafrost distribution determined from remote sensing of interior Alaska, USA. *Geophysical Research Letters*, 882-887.

Jorgenson, M. T., & Grosse, G. 2016. Remote sensing of landscape change in permafrost regions. *Permafrost and Periglacial Processes*, 324-338.

Jorgenson, M. T., Racine, C. H., Walters, J. C., & Osterkamp, T. E. 2001. Permafrost degradation and ecological changes associated with a warming climate in central Alaska. *Climatic Change 48*(4), 551-579.

Kääb, A. 2008. Remote sensing of permafrost-related problems and hazards. *Permafrost and Periglacial Processes* 107-136.

Kääb, A., Huggel, C., Fischer, L., Guex, S., Paul, F., Roer, I., & Weidmann, Y. 2005. Remote sensing of glacier- and permafrost-related hazards in high mountains: an overview. *Nat. Hazards Earth Syst. Sci. 5*, 527–554.

Kim, K., Lee, J., Ju, H., Jung, J. Y., Chae, N., Chi, J., . Kim, J.-S. 2021. Time-lapse electrical resistivity tomography and ground penetrating radar mapping of the active layer of permafrost across a snow fence in Cambridge Bay, Nunavut Territory, Canada: correlation interpretation using vegetation and meteorological data. *Geosciences Journal 25*, 877–890 .

Li, R., Li, Z., Han, J., Lu, P., Qiao, G., Meng, X., Zhou, F. 2021. Monitoring surface deformation of permafrost in Wudaoliang Region, Qinghai–Tibet Plateau with ENVISAT ASAR data, *International Journal of Applied Earth Observation and Geoinformation 104*, 102527.

Li, X., Jin, X., Wang, X., Jin, H., Tang, L., Li, X., He, R., …, & Zhang, S. 2021. Investigation of permafrost engineering geological environment with electrical resistivity tomography: A case study along the China-Russia crude oil pipelines. *Engineering Geology 291*, 106237.

Mustapha, A. 2013. Detecting surface water quality trends using Mann-Kendall tests and Sen's slope estimates. *International Journal of Agriculture Innovations and Research 1*, 108-114.

Muster, S., Langer, M., Abnizova, A., Young, K., & Boike, J. 2015. Spatio-temporal sensitivity of MODIS land surface temperature anomalies indicates high potential for large-scale land cover change detection in Arctic permafrost landscapes. *Remote Sensing of Environment 168*, 1-12.

Detection of Permafrost Degradation in Eastern Alaska Using Modis and Landsat Data (11672)
Kristie Hu (Canada), Yiping Chen (China, PR) and Sarah Fatholahi (Canada)

FIG Congress 2022
Volunteering for the future - Geospatial excellence for a better living
Warsaw, Poland, 11–15 September 2022

Natali, S. M., Schuur, E. A., & Rubin, R. L. 2011. Increased plant productivity in Alaskan tundra as a result of experimental warming of soil and permafrost. *Journal of Ecology 100*, 488-498.

Natali, S. M., Schuur, E. A., & Rubin, R. L. 2012. Increased Plant Productivity in Alaskan Tundra as a Result of Experimental Warming of Soil and Permafrost: Increased Plant Productivity in Alaskan Tundra. *Journal of Ecology 100*(2), 448-498.

Nguyen, T.-N., Burn, C. R., King, D. J., & Smith, S. L. 2009. Estimating the Extent of Near-surface Permafrost using Remote Sensing, Mackenzie Delta, Northwest Territories. *Permafrost and Periglacial Processes 20(2)*, 141 - 153.

Nill, L., Ullmann, T., Kneisel, C., Sobiech-Wolf, J., & Baumhauer, R. 2019. Assessing spatiotemporal variations of Landsat land surface temperature and multispectral indices in the Arctic Mackenzie Delta Region between 1985 and 2018. *Remote Sensing11(19)*, 2329.

Novikova, A., Belova, N., Baranskaya, A., Aleksyutina, D., Maslakov, A., Zelenin, E., & Ogorodov, S. 2018. Dynamics of permafrost coasts of Baydaratskaya Bay (Kara Sea) based on multi-temporal remote sensing data. *Remote Sensing 10(9)*, 1481.

Nyland, K. E., Gunn, G. E., Shiklomanov, N. I., Engstrom, R. N., & Streletskiy, D. A. 2018. Land cover change in the lower Yenisei River using dense stacking of Landsat imagery in Google Earth Engine. *Remote Sensing 10(8)*, 1226.

Panuju, D. R., Paull, D. J., & Griffin, A. L. 2020. Change detection techniques based on multispectral images for investigating land cover dynamics. *Remote Sensing 12(11)*, 1781.

Park, H., KimFollow, Y., & Kimball, J. S. 2016. Widespread permafrost vulnerability and soil active layer increases over the high northern latitudes inferred from satellite remote sensing and process model assessments. *Remote Sensing of Environment 175*, 349-358.

Pastick, N. J., Jorgenson, M. T., Wylie, B. K., Minsley, B. J., Ji, L., Walvoord, M. A., & Rose, J. R. 2013. Extending airborne electromagnetic surveys for regional active layer and permafrost mapping with remote sensing and ancillary data, Yukon Flats Ecoregion, Central Alaska. *Permafrost and Periglacial Processes 24(3)*, 1775.

Peng, X., Zhang, T., Frauenfeld, O. W., Wang, J., Qiao, L., Du, R., & Mu, C. 2019. Northern hemisphere greening in association with warming permafrost. *Journal of Geophysical Research: Biogeosciences 125*, e2019JG005086

Sarp, G., & Ozcelik, M. 2017. Water body extraction and change detection using time series: A case study of Lake Burdur, Turkey. *Journal of Taibah University for Science 11(3)*, 381-391.

Singh, K. V., Setia, R., Sahoo, S., Prasad, A., P., & Pateriya, B. 2015. Evaluation of NDWI and MNDWI for assessment of waterlogging by integrating digital elevation model and groundwater level. *Geocarto International 30(6)*, 650-661.

USGS. 2021. *Landsat Surface Reflectance-Derived Spectral Indices: Landsat Enhanced Vegetation Index.* https://www.usgs.gov/core-science-systems/nli/landsat/landsat-enhanced-vegetation-index, Retrieved 7 January 2022.

Detection of Permafrost Degradation in Eastern Alaska Using Modis and Landsat Data (11672)
Kristie Hu (Canada), Yiping Chen (China, PR) and Sarah Fatholahi (Canada)

FIG Congress 2022
Volunteering for the future - Geospatial excellence for a better living
Warsaw, Poland, 11–15 September 2022

USGS. 2021. *NDVI, the Foundation for Remote Sensing Phenology*, https://www.usgs.gov/special-topics/remote-sensing-phenology/science/ndvi-foundation-remote-sensing-phenology. Retrieved 7 January 2022.

Xu, H. 2006. Modification of normalised difference water index (NDWI) to enhance. *International Journal of Remote Sensing 27*(14), 3025-3033.

Zhang, C., Douglas, T. A., & Anderson, J. E. 2021. Modeling and mapping permafrost active layer thickness using field measurements and remote sensing techniques. *International Journal of Applied Earth Observation and Geoinformation 102*, 102455.

CONTACTS

Ms. Kristie Hu

Department of Geography & Environmental Management, University of Waterloo

200 University Avenue West, N2L 3G1

Waterloo, ON

Canada

(+1)519-729-5045

j265hu@uwaterloo.ca

Detection of Permafrost Degradation in Eastern Alaska Using Modis and Landsat Data (11672)
Kristie Hu (Canada), Yiping Chen (China, PR) and Sarah Fatholahi (Canada)

FIG Congress 2022
Volunteering for the future - Geospatial excellence for a better living
Warsaw, Poland, 11–15 September 2022